Thermal stability and spectroscopic properties of erbium-doped niobic-tungsten–tellurite glasses for laser and amplifier devices

Thermal stability and spectroscopic properties of erbium-doped niobic-tungsten–tellurite glasses for laser and amplifier devices

Nadia G. Boetti[a)*], Joris Lousteau[a)], Alessandro Chiasera[c)], Maurizio Ferrari[c)], Emanuele Mura[a)], Gerardo C. Scarpignato[a)], Silvio Abrate[b)], Daniel Milanese[a)]

[a)]*PhotonLab, Dipartimento di Scienza dei Materiali ed Ingegneria Chimica, Politecnico di Torino, Corso Duca degli Abruzzi 24, 10129, Torino, Italy.*
[b)]*PhotonLab, Istituto Superiore Mario Boella, Via P.C. Boggio, 61, 10138, Torino, Italy.*
[c)] *CNR-IFN, Istituto di Fotonica e Nanotecnologie, CSMFO Lab. via alla Cascata 56/C, Povo, 38123, Trento, Italy.*

*corresponding author. Tel: +39 0112276312, Fax: +39 0112276299. Email: nadia.boetti@polito.it.

ABSTRACT

Er^{3+} doped niobic-tungsten-tellurite glasses doped with concentration of Er^{3+} up to 3 wt% were fabricated. The effect of Er^{3+} doping concentration on thermal stability and optical properties was investigated in order to obtain the most suitable rare earth content for developing 1.5 μm compact fiber amplifier pumped with a commercial telecom 980 nm laser diode. The maximum doping concentration allowed was found to be around 1.77 x 10^{20} ions/cm^3, for which a broad 1.5 μm emission spectra of 65 nm FWHM and a lifetime of 3.4 ms for the $^4I_{13/2}$ level was measured.

KEYWORDS: Erbium, Niobic tungsten tellurite glass, Optical materials, Spectroscopic properties

INTRODUCTION

In order to increase the transmission capacity of wavelength-division-multiplexing (WDM) system it is important to flatten the gain spectrum and broaden the amplification bandwidth of erbium doped fiber amplifiers (EDFA's). A way to achieve this requirement is the employment of the tellurite-based erbium doped fiber amplifier (T-EDFA), that can provide a wide amplifying bandwidth in the 1530 nm region ($^4I_{13/2} \rightarrow {}^4I_{11/2}$ transition) due to its high stimulated emission cross-section [1]. Moreover tellurite glasses possess a number of advantages over conventional oxides glasses, such as a wide transmission bandwidth in the infrared wavelength region (up to 5 μm), good glass stability and corrosion resistance, high refractive index and high rare earth solubility [2].

EDFA for amplification of 1.5 μm signal can use both 980 nm and 1480 nm optical pumping. The 980 nm pumping scheme excites erbium ions from their ground-state level $^4I_{15/2}$ to the $^4I_{11/2}$, from where, in silica, there is a fast non-radiative relaxation to the level $^4I_{13/2}$. Due to that fast transfer, there is essentially no de-excitation via stimulated emission by pump light, and very high excitation levels can be achieved [3]; this allows obtaining the highest gain per unit length and lowest noise figure. However, in tellurite glasses, the relatively low phonon energy (< 800 cm^{-1}) makes the non-radiative relaxation rate between $^4I_{11/2}$ and $^4I_{13/2}$ too slow [4]; as a result its up-conversion fluorescence in the visible wavelength range is very strong [5] and, thus, pumping at 980 nm is inefficient.

On the other hand, the glass transition temperature of tellurite glass is also relatively low (about 300 °C), which makes it liable to thermal damage at high optical intensities.

To overcome these two drawbacks different compound tellurite based glasses have been investigated including tungsten-tellurite [6, 7], boro-tellurite [8], germano-tellurite [9], niobium-tellurite [10, 11, 12, 13], phospho-tellurite [14, 15], and niobium-tungsten-tellurite [16, 17].

In this paper we report the study of thermal stability and spectroscopic properties of Er^{3+} doped niobium-tungsten-tellurite glasses because tungsten oxide and niobium oxide can be incorporated simultaneously in the tellurite glass network and both increase the glass thermal stability and phonon energy [6, 13].

The effect of Er^{3+} doping concentration on optical properties is investigated in order to obtain the maximum doping level allowed without concentration quenching effect.

This work is intended to be a preliminary study towards the realization of a compact broadband EDFA pumped with a commercial telecom 980 nm laser diode. Another interesting use of highly erbium doped tellurite optical fibers is for compact eye-safe fiber lasers to be installed on vehicles, aircrafts and satellites for environmental monitoring and sensing.

2. EXPERIMENTAL PROCEDURE

2.1 Samples preparation

Glass samples (35g batch) used in this research were prepared using chemicals of 99+% purity. Molar composition of the fabricated samples was as follows: $68.2TeO_2$:$22.1WO_3$:$7Na_2O$:$2.6Nb_2O_5$, doped with x added wt% of Er_2O_3 (x = 0.01, 0.1, 0.5, 1, 3). The samples were named as TWNNb3 ÷ TWNNb7 for short. After weighting and mixing, the batched chemicals were transferred into a platinum crucible for melting within a chamber furnace. The melting procedure was carried out inside a glove box under dried air atmosphere with a water level lower than 0.1 ppmv. The onset melting temperature was 730 ˚C and the duration of the process 2 hours. The melt was cast into a brass mould

preheated and annealed at T_g – 10 °C for 2 h. The obtained glasses were cut and optically polished with a diamond paste to 2 mm thick samples for different optical and spectroscopic characterization.

2.2 Property measurements

Density of samples was measured by Archimedes method using distilled water as immersion fluid. The Er^{3+} ion concentrations were calculated from measured sample densities and their initial compositions.

Thermal analysis was performed on fabricated glasses using a Perkin Elmer DSC-7 differential scanning calorimeter up to 550°C under Ar flow with a heat rate of 10°C/min in sealed Al pans using typically 30 mg samples. Thermal analysis was carried out in order to measure the characteristic temperatures T_g (glass transition temperature) and T_x (onset crystallization temperature). Their measurement allowed assessing the corresponding glass stability $\Delta T = T_x - T_g$ that is an estimation of the fiber drawing ability of the glasses. In fact larger ΔT, for a glass host, means larger working range during sample fiber drawing. An error of ±3 °C was observed in measuring the characteristic temperatures.

The refractive index of the glasses was measured at 1.3 μm, where Er^{3+} ions do not display ground state absorption, by prism coupling technique (Metricon, model 2010). Ten scans were used for each measurement. Estimated error of the measurement was ±0.001.

The absorption spectra were measured at room temperature for wavelength ranging from 350 to 3000 nm using a double beam scanning spectrophotometer (Varian Cary 500).

CW photoluminescence for emission ranging from 1400 to 1700 nm were recorded by exciting the samples with the 514.5 nm line of a Argon ion laser and dispersing the light by a 320 mm single-grating monochromator. The light was detected by a NIR photomultiplier tube (Hamamatsu H9170-75) and standard lock-in technique.

The fluorescence lifetime of Er^{3+}:$^4I_{13/2}$ level was obtained by chopping the CW exciting beam with a mechanical chopper, recording the signal by a digital oscilloscope (Tektronix TDS350) and fitting the decay traces by single exponential.

Lifetime measurements of Er^{3+}:$^4I_{13/2}$ and $^4I_{11/2}$ were also obtained by exciting the samples with light pulses of 978 nm single mode fiber pigtailed laser diode.

All measurements were performed at room temperature.

3. RESULTS AND DISCUSSIONS

3.1 Physical and thermal properties

Thermal properties, density, refractive index and the calculated Er^{3+} ion concentration of fabricated glasses are reported in Table 1.

The glass transition temperature was found to increase monotonically with Er^{3+} content. A minimum glass stability value of 163 °C was obtained for an Er^{3+} concentration of 1.80 x 10^{19} ions/cm^3, sample TWNNb4, while the most stable glass compositions TWNNb3 shows a stability parameter of 182 °C. These results demonstrate that these TWNNb glasses are very stable against de-vitrification and suitable for fiber drawing.

Glass density increased with Er^{3+} ion concentration. Absolute values are in agreement with the results made with the same method on similar glass compositions [16, 17].

The refractive index of the glasses decreased with increasing Er^{3+} ion content.

3.2 Absorption spectra

UV–VIS–NIR spectroscopy was carried out on all prepared samples and absorption spectra were recorded. Absorption cross-section σ_a was calculated from experimental data using the following formula:

$$\sigma_a(\lambda) = \frac{2.303 \log\left(\frac{I_0}{I}\right)}{NL}$$

where $log(I_0/I)$ is the absorbance, L the glass sample thickness in cm and N is the concentration of the Er^{3+} ions per cm^3. Fig. 1 shows the absorption cross-section values obtained for glass sample TWNNb7. The inhomogeneously broadened bands are assigned to the transitions from the ground state $^4I_{15/2}$ to the excited states of Er^{3+} ions (inset of Fig. 1).

3.3 Fluorescence emission spectra

Fig. 2 illustrates the fluorescence spectra in the wavelength range 1400÷1700 nm under 514.5 nm excitation. The broad 1.53 μm emission is assigned to the $^4I_{13/2} \rightarrow {}^4I_{15/2}$ transition. The shape of the band shows, compared to tellurite glass, a spectral broadening at longer wavelength due to the presence in these glass samples of two network formers, TeO_2 and WO_3 and thus the existence of two types of dopant site. The resultant emission spectrum is then inhomogeneously broadened by combined contributions from all sites and it is similar to that observed in other tungsten-tellurite glasses [6, 18].

Fig. 3 reports the peak height of the 1.53 μm emission and the emission full-width at half maximum (FWHM) with respect to the Er^{3+} ion concentration. It can be observed that the peak emission intensity increases steadily with rising doping concentration, due to the increasing absorption of pump source at the beginning stage. But when Er^{3+} concentration becomes higher than 1.77 x 10^{20} ions/cm^3 the absorption saturation of pump source is approached and the rate of the increase of emission intensity decreases. Moreover, for high Er^{3+} ions concentration, the up-conversion emission becomes stronger and this reduces the population of the $^4I_{13/2}$ level.

Because of the difference in the emission spectra of different glass hosts, the FWHM is often used as a semi-quantitative indicator of the bandwidth. In the fabricated samples, it ranges from 50 to 65 ± 2 nm, similar to other tungsten [7] and niobium [11] tellurite glasses and larger than those of aluminium-silicate glasses (40 nm in [19]) and phosphate glasses (37nm in [20]). In Fig. 3 it can be seen that FWHM becomes higher as Er^{3+} ion concentration increases up to 1.77 x 10^{20} ions/cm^3, while for higher concentration it is almost unchanged. This broadening trend can be due to radiative trapping, which generally occurs in a typical 3-level system when the absorption and fluorescence spectra overlap, as already observed in [21].

3.4 Fluorescence lifetime

Another experimental parameter required to characterize the emission properties of rare-earth ions in a host medium, and therefore its suitability for active optical devices, is the fluorescence lifetime. In particular for optical amplifiers or lasers at the 1.55 μm band, the important parameter is the $^4I_{13/2}$ lifetime: the longer the lifetime the higher the population inversion between this level and the ground state.

The decay curves of the $^4I_{13/2}$ and $^4I_{11/2}$ were measured upon 514.5 nm excitation for all samples. Examples of the measured curves are reported in Fig. 4. Measurements of the decay curve of $^4I_{13/2}$ were also repeated under excitation at 978nm. Lifetimes values were calculated for all samples and are reported in Tab. 2.

The obtained lifetime values as a function of the Er^{3+} ion concentration are reported in Fig. 5. The $^4I_{13/2}$ lifetime trend is similar to that observed in other tungsten-tellurite glasses: initially lifetime increases with rising concentration then, for

higher doping level, lifetime decreases due to the effect of concentration quenching. The initial increase has been already reported [6] and can be explained by the effect of radiation trapping [22].

The longest lifetime of 3.7 ± 0.2 ms was measured for the sample TWNNb5, i.e. for Er^{3+} doping level of 8.9 x 10^{19} ions/cm^3. This value is higher than other Nb-doped glasses [12] with similar Er^{3+} ions content: the reason is probably due to a lower niobium oxide content in our case, together with the use of controlled dry atmosphere for melting.

When pumped by a 978 nm diode laser, Er^{3+} ion is excited to the $^4I_{11/2}$ level then it rapidly relaxes to the $^4I_{13/2}$ through non radiative decay. The rate of this relaxation is very important for creating population inversion of $^4I_{13/2}$ level for optical amplification at 1.5 μm. Our measured lifetime of the $^4I_{11/2}$ level of Er^{3+} is 140 ± 30 μs, which is much smaller than the lifetime (290 ± 30 μs) we measured in $75TeO_2$:17ZnO:$8Na_2O$ glass [23] or than the value measured in [4]. The observed increase of the relaxation decay rate is due to the efficiency of the non-radiative transition rate on the relaxation dynamic from the $^4I_{11/2}$ state [24] in the case of niobic-tungsten-tellurite glasses. In fact, incorporation of tungsten oxide and niobium oxide in the tellurite glass increase the cut-off phonon energy at about 920 cm^{-1} with respect to the 800 cm^{-1} of zinc tellurite glasses [25]. The corresponding energy gap between the $^4I_{11/2}$ and $^4I_{13/2}$ electronic states of the Er^{3+} ion is about 3300 cm^{-1} and the $^4I_{11/2}$ non radiative relaxation rate can be estimated following the well established theory of Layne, Lowdermilk, and Weber [24]. For the investigated glass a multiphonon decay rate in the order of 1x10^5 sec^{-1} is obtained in respect to 0.5x10^5 sec^{-1} of tellurite glasses. So, unlike tellurite glass where such pumping is highly inefficient, niobium-tungsten-tellurite glasses allow more efficient EDFA pumping at 980 nm.

4. CONCLUSION

Thermal stability and spectroscopic properties of Er^{3+} doped niobic-tungsten-tellurite glasses were measured. The effect of Er^{3+} doping concentration on optical properties was investigated in order to obtain the maximum doping level allowed without concentration quenching effect. The 1.5 μm emission band became broader with increasing the concentration of Er^{3+} ions. FWHM ranges from 50 to 65 ± 2 nm at concentration of Er^{3+} ions corresponding to 0.18 and 51.5 x 10^{19} ions/cm^3, respectively. The lifetime of the $^4I_{13/2}$ state decreased with increasing Er^{3+} concentration due to energy transfer process. The lifetime of the $^4I_{11/2}$ state of Er^{3+} remained unchanged with the increase of Er^{3+} concentration and short enough to allow EDFA pumping at 980 nm. Moreover, as an important finding of this study we mention the role of tungsten oxide and niobium oxide on the increase of the cut-off phonon energy leading to a fast filling of the $^4I_{13/2}$ state by efficient non-radiative relaxation from the next upper $^4I_{11/2}$ Er^{3+} multiplet. The maximum doping concentration allowed is around 1.77 x 10^{20} ions/cm^3, i.e. sample TWNNB6, for which a broad 1.5 μm emission spectra of 65 nm FWHM and a lifetime of 3.4 ms for the $^4I_{13/2}$ level was measured. Hence the TWNNB6 is the chosen sample to be used for the realization of a compact broadband EDFA pumped with a commercial telecom 980 nm laser diode.

ACKNOWLEDGMENTS

The authors acknowledge the support of Regione Piemonte through the Converging Technologies “Hipernano” research project. Authors recognize the invaluable technical assistance of E. Moser (University of Trento), A. Carpentiero (IFN-CNR), and S. Varas (IFN-CNR).

REFERENCES

[1] Y.O. Mori, and S. Sudo, Electron. Lett. 33, 863 (1997).
[2] J.S. Wang, E.M Vogel, and E. Snitzer, Opt. Mat. 3, 187 (1994).
[3] R. I. Laming, M. C. Farries, P. R. Morkel, L. Reekie, D. N. Payne, P. L. Scrivener, F. Fontana, and A. Righetti, Electron. Lett. 25, 12 (1989).
[4] D.H. Cho, Y.G. Choi, K.H. Kim, ETRI Journal 23, 4, 151, (2001).
[5] G.A.Kumar, E. De La Rosa, H. Desirena, Optics Communications, 260 (2), 601, (2006).
[6] S. Shen, M. Naftaly and A. Jha, Optics Communications, 205, 101, (2002).
[7] S. Zhao, X. Wang, D. Fang, S. Xu, and L. Hu, J. Alloys Compd, vol. 424, pp. 243-246, (2006).
[8] S. Hocde, S.B. Jiang, et al., Opt. Mater., 25 (2), 149, (2004).
[9] X. Feng, S. Tanabe, T. Hanada, J. Am. Ceram. Soc., 84, 165, (2001).
[10] M. V. D. Vermelho, A. S. Gouveia-neto, and H. T. Amorim, J. Lumin., vol. 103, pp. 755-761, (2003).
[11] D. D. Chen, Y. H. Liu, Q. Y. Zhang, Z. D. Deng, and Z. H. Jiang, Mater. Chem. Phys., 90, 78-82, (2005).
[12] S. Dai, J. Wu, J. Zhang, G. Wang, and Z. Jiang, Spectrochim. Acta Part A, vol. 62, pp. 431-437, (2005).
[13] F. C. Cassanjes, Y. Messaddeq, L. F. C. D. Oliveira, and L. C. Courrol, J. Non-Cryst. Solids, vol. 247, pp. 58-63, (1999).
[14] T. Toney Fernandez, S. M. Eaton, G. Della Valle, R. Martinez Vazquez, M. Irannejad, G. Jose, A. Jha, G. Cerullo, R. Osellame, and P. Laporta, Opt. Express, 18**,** 20289, (2010).
[15] P. Nandi and G. Jose, Opt. Comm., 265**,** 588, (2006).
[16] S. Xu, S. Dai, J. Zhang, L. Hu, Z. Jiang, Chin. Opt. Lett., 2, 106, (2004).
[17] X. Wang, Spectrochim. Acta Part A, 70, 99–103, (2008).
[18] Y. Luo, J. Zhang, J. Sun, S. Lu, X. Wang, Opt. Mat., 28, 255–258, (2006).
[19] W.J. Miniscalco, in: M.J.F. Digonnet (Ed.), Rare Earth Doped Fiber Lasers and Amplifiers, Marcel Dekker, New York, p. 19, (1993).
[20] S. Jiang, T. Luo, B.C. Hwang, J., Non-Cryst. Solids, 263–264, 364, (2000).
[21] S. Dai**,** C. Yu, G. Zhou, J. Zhang, G. Wang and L. Hu, J. of Lumin Volume 117, Issue 1, 39-45, (2006).
[22] F. Auzel, G. Baldacchini, L. Laversenne, G. Boulon, Opt. Mat., 24, 103–109, (2003).
[23] J. Losteau, N. Boetti, A. Chiasera, M. Ferrari, S. Abrate, G. Scarciglia, A. Venturello, D. Milanese "Er3+ and Ce3+ co-doped tellurite optical fiber for lasers and amplifiers in the near infrared wavelength region: fabrication and optical characterization" Submitted IEEE Photonics J..
[24] C.B. Layne, W.H. Lowdermilk, and M.J. Weber, Phys. Rev. B, 16, 10, (1997).
[25] N. Jaba, A. Mermet, E. Duval, B. Champagnon, J. Non-Cryst. Solids, 351, 833, (2005).

FIGURES

Fig. 1. Absorption cross-section spectrum for sample TWNNB7. The main Er^{3+} levels are labeled, considering absorption from the ground state $^4I_{15/2}$. The inset shows Er^{3+} ion energy levels.

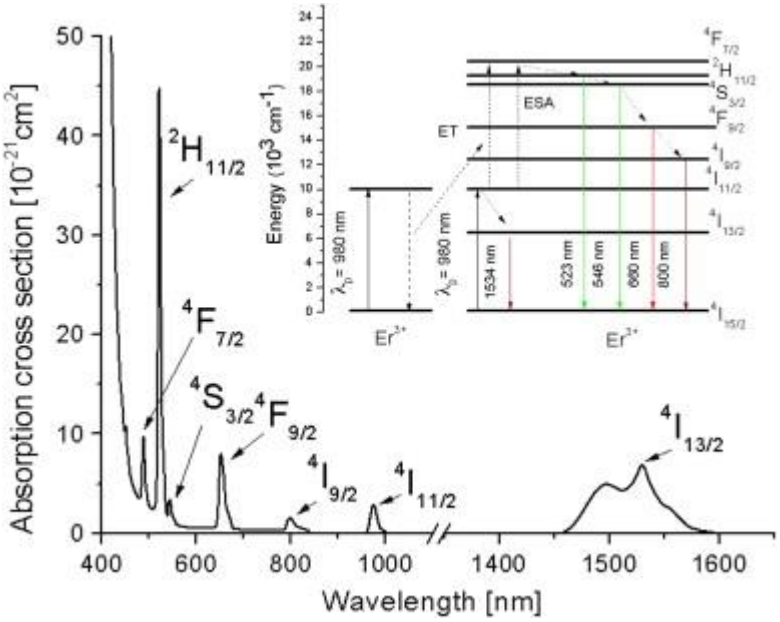

Fig. 2. Emission spectra of the $^4I_{13/2} \rightarrow {}^4I_{15/2}$ transition of Er^{3+} upon 514.5 nm excitation for the fabricated glass samples.

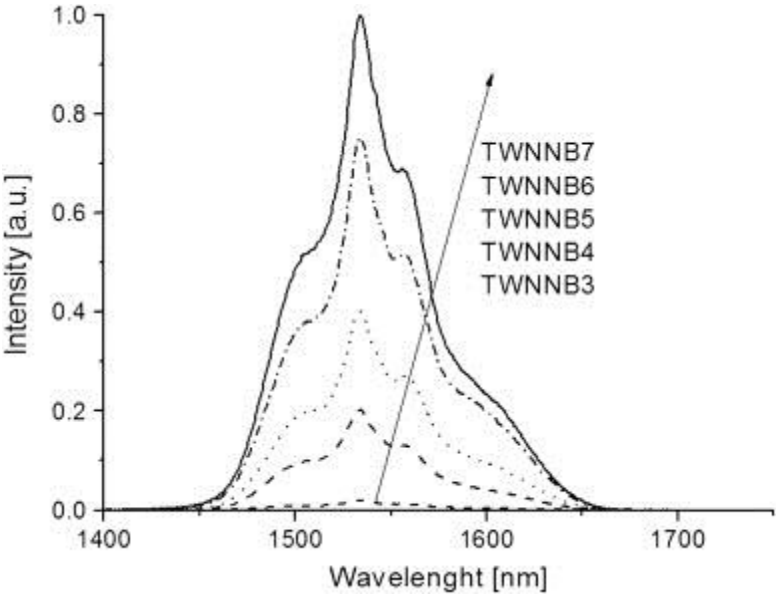

Fig. 3. Dependence of peak height and FWHM of the $^4I_{13/2} \rightarrow {}^4I_{15/2}$ transition on the Er^{3+} ion concentration

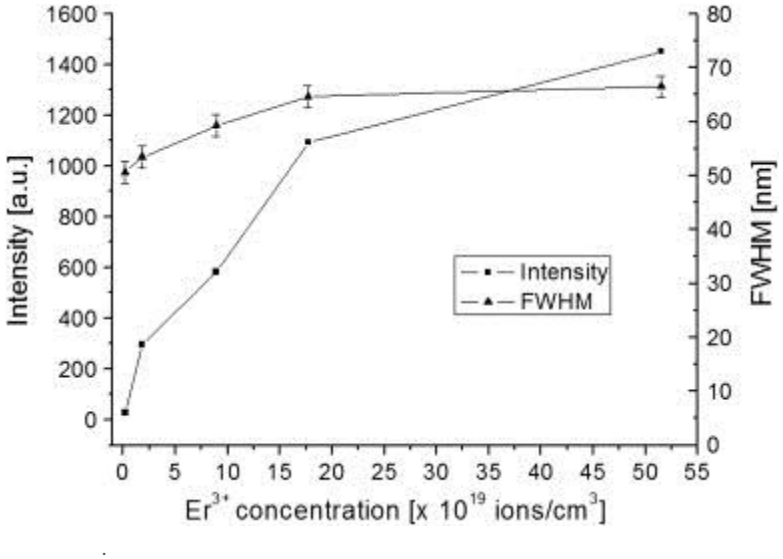

Fig. 4. Room temperature decay curves of the $^4I_{13/2}$ (a) and $^4I_{11/2}$ (b) level of Er^{3+} ions in two different samples obtained upon excitation at 514.5 nm. The intensity data are reported on a Log scale.

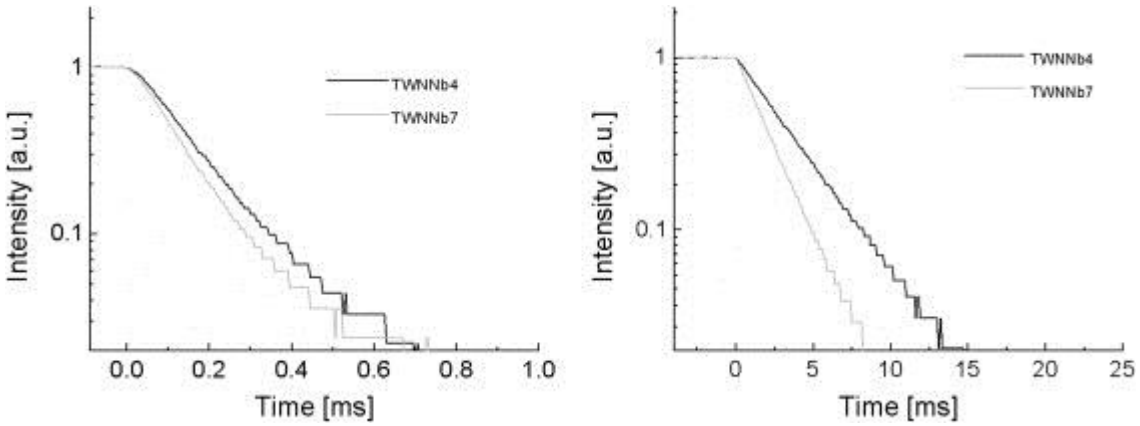

Fig. 5. Dependence of excited state lifetime values on the Er^{3+} ion concentration.

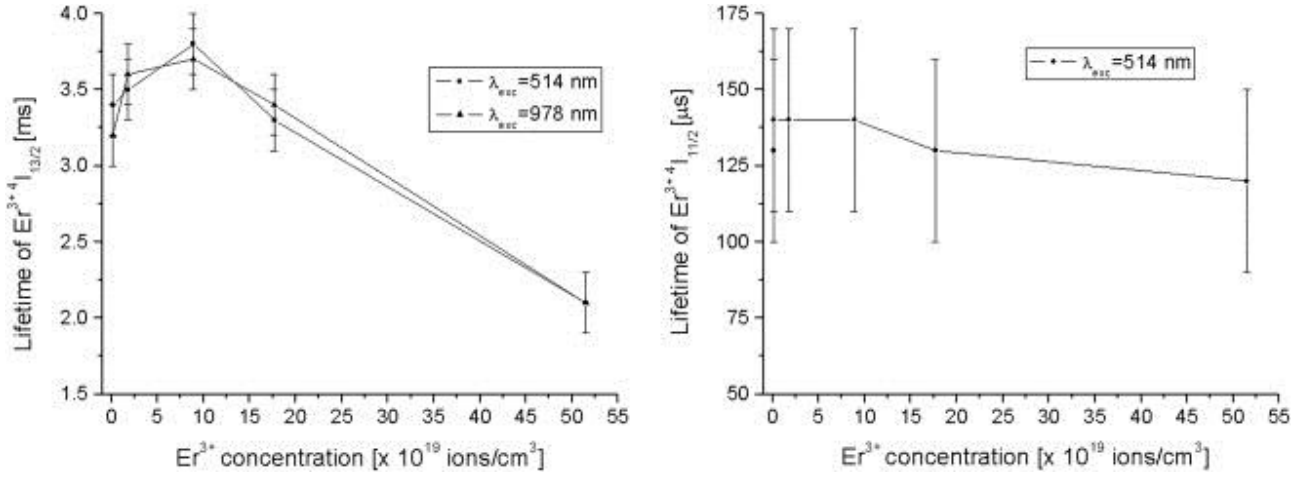

TABLES

Table 1. Er^{3+} ion content in wt%, Er^{3+} ion concentration, glass transition temperature (T_g), crystallization temperature (T_x), density, and refractive index of the manufactured tellurite glasses.

Glass label	Er^{3+}[wt%]	Er^{3+} [x 10^{19}ions/cm^3]	T_g [°C] ±3 °C	T_x [°C] ±3 °C	$\Delta T = T_x - T_g$ [°C]± 6 °C	ρ [g/cm^3]± 0.05 g/cm^3	n± 0.001
TWNNb3	0.01	0.18	*365*	*547*	182	5.70	*2.068*
TWNNb4	0.1	1.80	*368*	*531*	163	5.72	*2.066*
TWNNb5	0.5	8.90	*371*	*540*	169	5.71	*2.067*
TWNNb6	1	17.7	*370*	*540*	170	5.73	*2.064*
TWNNb7	3	51.5	*379*	*552*	173	5.74	*2.059*

Table 2. Excited state lifetime values for Er^{3+} doped samples under laser excitation at 514.5 nm and 980 nm.

Glass label	Er^{3+}[wt%]	Er^{3+}:$^4I_{13/2}$ lifetime [ms] ±0.2 ms		Er^{3+}:$^4I_{11/2}$ lifetime [µs] ±30 µs
		λ_{exc}=514.5 nm	λ_{exc}=978 nm	λ_{exc}=514.5 nm
TWNNb3	0.01	3.2	3.4	140
TWNNb4	0.1	3.6	3.5	140
TWNNb5	0.5	3.7	3.8	140
TWNNb6	1	3.4	3.3	130
TWNNb7	3	2.1	2.1	120